CHAPTER 1

INTRODUCTION

1.1 BACKGROUND AND MOTIVATION

Orthogonal frequency division multiplexing (OFDM) has become a very popular method for high-data-rate communication, primarily because of its tight spectral efficiency and its robustness to multi-path fading. This has led to it being deployed in various standards, such as digital subscriber lines, digital video broadcasting (DVB), digital radio mondiale (DRM), worldwide inter-operability for microwave access (WiMAX) IEEE 802.16d standard, wireless fidelity (Wi-Fi) IEEE 802.11n standard and recently in long-term evolution (LTE). However, it is a well-known that OFDM is plagued by a large peak-to-average power ratio (PAPR) problem. This high PAPR occurs when the sinusoidal signals of the sub-carriers are added constructively. This results in a signal which consists of a number of infrequent peaks. This signal with infrequent peaks needs to be amplified before transmission through a channel. The irregularity of these peaks leads to inefficient use of the power amplifiers, amongst other things, which ultimately reduces the battery life of the mobile device, which is undesirable.

This has resulted in various methods being developed to reduce the PAPR of an OFDM transmission. These are clipping, decision-aided reconstruction clipping, coding, partial transmission sequence, selective mapping, companding transforms, active constellation extension (ACE), tone reservation and constant envelope OFDM phase modulation, amongst

others. However, these methods require high implementation complexity, additional bandwidth expansion or the transmission of side information to reconstruct the original message signal. Some of these methods also result in an average power increase, or lead to a severe bit error rate (BER) degradation as the number of carriers increases. Ideally a PAPR method which does not result in a number of the drawbacks that are being experienced by current methods in the field is required. In this thesis, such a method, called offset modulation, is proposed.

1.2 AUTHOR'S CONTRIBUTION AND OUTPUTS

1.2.1 Research contributions

The author's main research contribution can be summarised as follows

- A novel method called offset modulation (OM-OFDM) has been proposed to control the PAPR of an OFDM transmission for a targeted BER. The theoretical bandwidth occupancy of the proposed offset modulation signal was derived. Using these bandwidth occupancy results, a closed-form theoretical BER expression for an offset modulation transmission was derived and validated.

- A newly applied decision metric (D) has been introduced, which can be utilised throughout the PAPR field to compare various methods.

- An offset modulation with active constellation extension (OM-ACE) method has been proposed to control the PAPR of an OFDM transmission for a targeted BER. A closed-form BER expression for this OM-ACE transmission is presented and validated.

- A theoretical generic closed-form relationship between the probability of a missed detection (P_{md}) and the probability of a false alarm (P_{fa}) for any unknown deterministic signal (for instance OFDM and OM-OFDM) has been derived and validated.

- The receiver operating characteristic curves, which relate P_{md} to the P_{fa} for both a typical DVB-T2 OFDM and OM-OFDM transmission is presented.

1.2.2 Patents

The current patents that have been filed as outputs of this research are

- K. Dhuness and B. T. Maharaj, “An offset modulation scheme to control the PAPR of a signal", SA Patent, No. 2010/03368, provisional, May 2010.
- K. Dhuness and B. T. Maharaj, “Modulation of Signals", provisional - PCT/IB2011/052066, USPTO, May 2011.

1.2.3 Publications

The research as reflected in this thesis was partially based on the following conference and journal articles, published by the author

- K. Dhuness and B. T. Maharaj, “Comparative performance of OM-OFDM in broadband systems," Electronics Letters, vol 48, issue 2, pp. 127-129, January 2012.
- K. Dhuness and B. T. Maharaj, “A cognitive radio application of OM-OFDM," in Proceedings of the IEEE Africon, Livingston, Zambia, 13-15 September 2011, pp. 1-5. **Outstanding paper award**
- K. Dhuness and B. T. Maharaj, “An Offset Modulation scheme to control the PAPR of an OFDM transmission," in Proceedings of the IEEE 72nd Vehicular Technology Conference, Ottawa, Canada, 6-9 September 2010, pp. 1-5. **Invited paper**
- K. Dhuness, P. Botha and B. T. Maharaj, “A decision metric approach to PAPR performance analysis of an OM-OFDM transmission," in Proceedings of the Southern Africa Telecommunication Network and Application Conference, Stellenbosch, South Africa, 5-8 September 2010, pp. 1-6.

Two ISI accredited journal articles based on this work are currently under review.

1.3 OUTLINE OF THESIS

In Chapter 2, the OFDM concept is introduced and the origin of the PAPR problem associated with an OFDM transmission is presented. Various PAPR reduction methods in the field are discussed, and the drawbacks of these methods are presented.

An offset modulation method is developed in Chapter 3, which does not result in a number of the drawbacks experienced by current methods in the field. A closed-form bandwidth occupancy expression and BER expression for an OM-OFDM transmission is derived. Thereafter a newly applied power performance decision metric is introduced. This metric can be utilised throughout the PAPR field to compare various PAPR methods.

The proposed OM-OFDM method may appear to be similar if not identical to a well-known constant envelope OFDM phase modulation (CE-OFDM) method. In Chapter 4, the significant modulation and structural differences between an OM-OFDM and a CE-OFDM method are discussed. The OM-OFDM, OFDM and CE-OFDM methods are compared by using a BER analysis and the newly applied decision metric.

In Chapter 5, the proposed OM-OFDM method is compared to OFDM, as well as various other PAPR reduction methods, by utilising a power performance decision metric and a complementary cumulative distribution function, after which conclusions are drawn.

The author demonstrates, in Chapter 6, the ease with which an ACE method, which is a well-established PAPR reduction method, may be incorporated into an OM-OFDM transmission, resulting in an OM-ACE method. The proposed OM-ACE method is developed; thereafter the bandwidth occupancy of an OM-ACE transmission is introduced. The reasoning for the inclusion of the ACE method into an OM-OFDM transmission is discussed and a closed-form BER expression for an OM-ACE transmission is also presented. Thereafter the OFDM, clipped OFDM, OM-ACE and ACE methods are compared by using a BER performance analysis, power performance decision metric and complementary cumulative distribution function and conclusions are drawn.

In Chapter 7, the cognitive radio applications of OM-OFDM are investigated by studying the ability of a secondary user to detect OM-OFDM and OFDM transmissions. The receiver operating characteristic (ROC) expression for any unknown signal is derived and validated. The ROCs of OM-OFDM and OFDM transmissions are investigated, and conclusions are drawn.

Based on all these results, Chapter 8 summarises the conclusions of the various chapters and suggests opportunities for further research.

CHAPTER 2

ORTHOGONAL FREQUENCY DIVISION MULTIPLEXING

2.1 INTRODUCTION TO OFDM

In order to understand OFDM, it is useful to discuss frequency division multiplexing (FDM). In a FDM system [1], depicted in Fig. 2.1, multiple signals are transmitted simultaneously (in the same time slot) over different frequencies. Each sub-carrier contains different data streams and guard bands are used between sub-carriers to avoid inter-signal over-

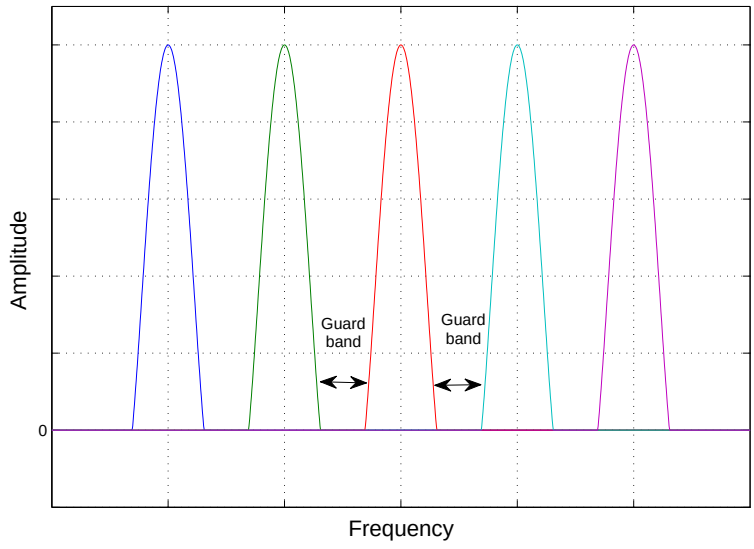

Figure 2.1: Frequency division multiplexing

lap/interference. Pulse-shaping filters are used to eliminate the inter-sub-carrier harmonics and thus eliminate inter-signal interference. Like FDM, OFDM [1] also uses multiple sub-carriers, but these sub-carriers are closely spaced to each other, depicted in Fig. 2.2, without causing inter-signal interference. This is possible because, as depicted in Fig. 2.2, the sub-carriers are orthogonal to each other, i.e. the peak of each sub-carrier coincides with the null of an adjacent sub-carrier. This type of orthogonal spacing removes the guard bands between adjacent sub-carriers and the subsequent inter-signal interference. A comparison between

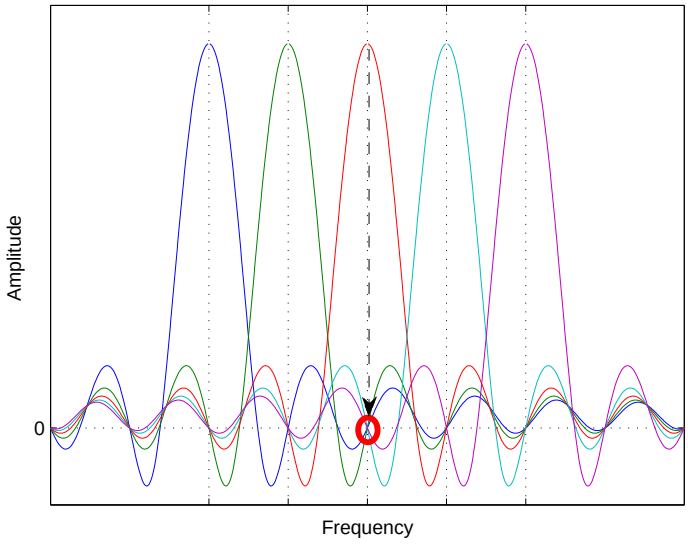

Figure 2.2: Orthogonal frequency division multiplexing

Fig. 2.1 and Fig. 2.2 indicates that OFDM requires less bandwidth than FDM, while transmitting the same amount of information. This translates to better spectral efficiency.

2.2 OFDM TRANSMITTER

In Fig. 2.3 an OFDM transmitter structure is presented. During an OFDM transmission [2], depicted in Fig. 2.3, binary input data are mapped (e.g. by using 4-QAM constellation) to complex symbols. These symbols undergo a serial-to-parallel conversion; thereafter pilot symbols are inserted. These pilot symbols will later be used by the equaliser to mitigate the effects of the channel. The subsequent symbols are passed through an inverse fast Fourier transform (IFFT), which places the complex input symbols orthogonal to each other. Part

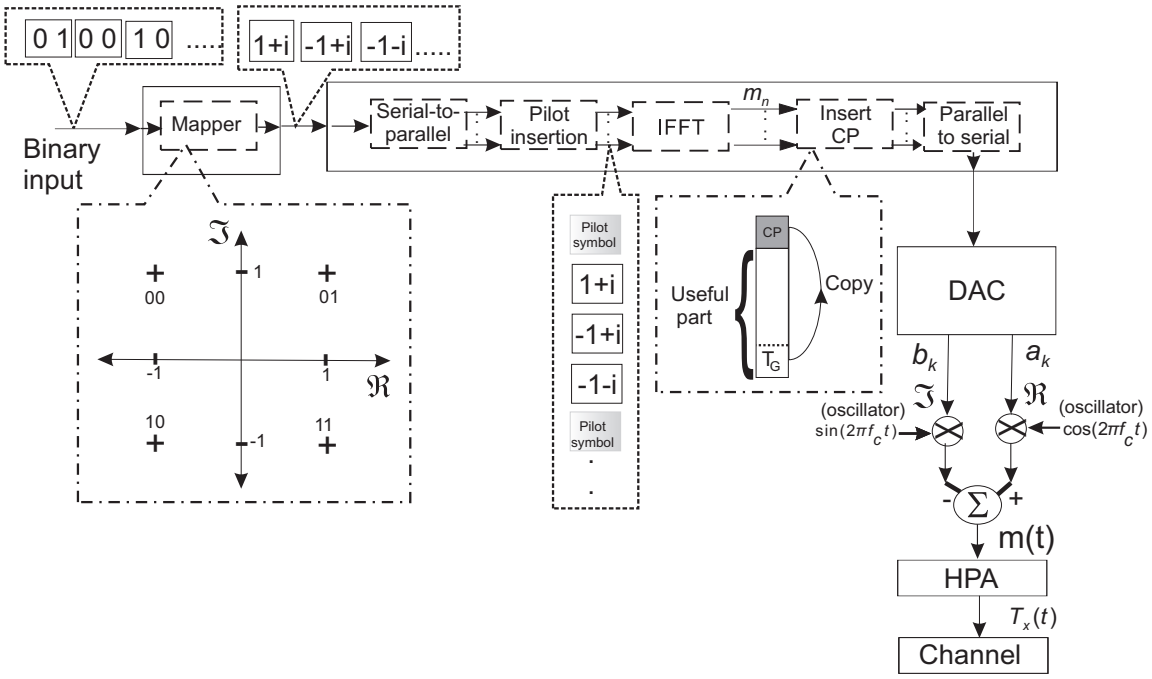

Figure 2.3: Orthogonal frequency division multiplexing transmitter structure

of the end of the resultant IFFT output (T_G guard interval) is copied and amended to the beginning of the signal. This process is referred to as adding a cyclic pre-fix (CP) or guard interval. This guard interval is used to mitigate some of the effects caused by multiple reflected, and delayed versions of the originally transmitted signal arriving at the receiver. The CP-amended IFFT output undergoes a parallel-to-serial conversion and is thereafter passed through a digital-to-analog converter (DAC). The subsequent real and imaginary components of the signals are modulated by using a sinusoid and co-sinusoid oscillator. The resultant real and imaginary modulated signals are combined and passed through a high-power amplifier (HPA).

This process can be mathematically explained, by considering that the IFFT is a transformation which maps the complex input data symbols (e.g. 4-QAM constellation symbols) $[x_0, x_1, ..., x_{N-1}]$ to OFDM symbols $[X_0, X_1, ..., X_{N-1}]$ such that the complex baseband

OFDM signal is given by [3]

$$m_n = \frac{1}{\sqrt{N}} \sum_{k=0}^{N-1} X_k e^{j\frac{2\pi nk}{N}}, \qquad n = 0,1,.....,N-1 \tag{2.1}$$

where N refers to the N-point IFFT and X_k represents the complex signal output $(a_k + jb_k)$ of the IFFT. The $e^{j\frac{2\pi nk}{N}}$ expression in Eq (2.1) uniformly spaces the OFDM $[X_0, X_1, ..., X_{N-1}]$ symbols. Thereafter, as depicted in Fig. 2.3, a CP or guard interval is amended to the resultant complex base band OFDM signal $\{X_v, n = 0,1....,N-1\}$, where the first X_v samples constitute the CP prefix. The CP is amended to the baseband OFDM signal between $n = -v,...,0$. As depicted in Fig. 2.3, this results in the signal in the $n = N-v, N-v+1,.....,N-1$ interval being placed in the $n = -v,-v+1,...,0$ interval [3]. The output of this CP block undergoes a parallel-to-serial conversion and is fed into a DAC. Thereafter the real and imaginary components are modulated by using an oscillator. The subsequent carrier frequency signal is then written as

$$\begin{aligned} m(t) &= \frac{1}{\sqrt{N}} \Re\left\{ \sum_{k=0}^{N-1} X_k e^{j2\pi t(f_c + \frac{k}{T_s})} \right\}, \qquad 0 \le t < T_s \\ &= \frac{1}{\sqrt{N}} \Re\left\{ \sum_{k=0}^{N-1} X_k e^{j(2\pi f_c t + \omega_k t)} \right\}. \end{aligned} \tag{2.2}$$

Here, $\Re\{.\}$ refers to the real components, T_s is the signal duration, f_c is the carrier frequency and $\omega_k = \frac{2\pi k}{T_s}$ are the subcarrier frequencies. After applying an Euler transform to Eq (2.2), the transmitted carrier frequency signal may be written as

$$\begin{aligned} m(t) &= \frac{1}{\sqrt{N}} \Re\left\{ \sum_{k=0}^{N-1} (a_k + jb_k)(\cos(2\pi f_c t + \omega_k t) + j\sin(2\pi f_c t + \omega_k t)) \right\} \\ &= \frac{1}{\sqrt{N}} \sum_{k=0}^{N-1} a_k \cos(2\pi f_c t + \omega_k t) - b_k \sin(2\pi f_c t + \omega_k t). \end{aligned} \tag{2.3}$$

The resultant signal $m(t)$ is amplified, by passing it through a HPA. In the case of a linear amplification process, the output can be written as

$$T_x(t) = A \cdot m(t). \tag{2.4}$$

In Eq (2.4), *A* refers to the amplification factor. The subsequent amplified OFDM signal is then transmitted through a channel.

2.3 OFDM TRANSMISSION

There are many kinds of channel interferences in wireless communication. A typical transmission might experience multi-path fading, depicted in Fig. 2.4(a), consisting of a direct path and two reflections. This type of channel interference is typically represented, as shown in Fig. 2.4(b), by a power delay profile (PDP). The PDP [4], in Fig. 2.4(b), represents each path (including amplitude degradation) of a transmission and the subsequent path delays (τ_0, τ_1 and τ_2), introduced by the channel. The purpose of the CP inclusion in Fig. 2.3

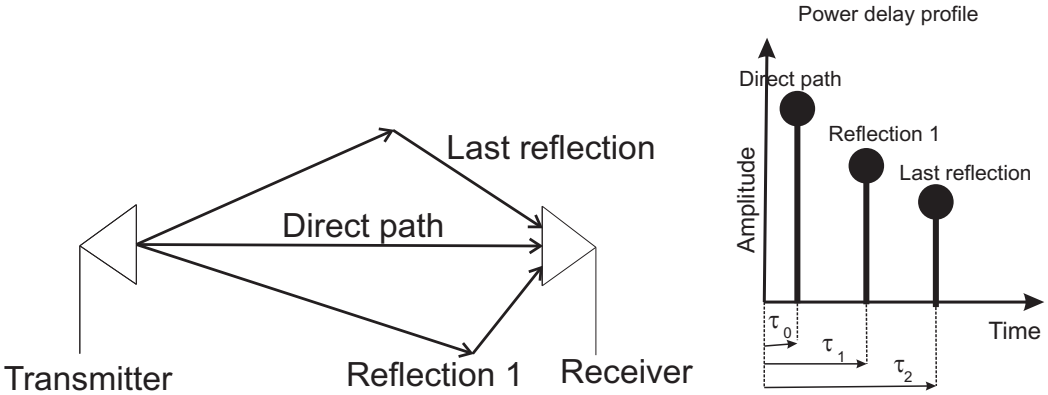

(a) 3-ray channel effects (b) 3-Tap power delay profile

Figure 2.4: Typical channel

is to mitigate some of the channel effects. The multi-path channel, depicted in Fig. 2.4(a), causes direct and multiple reflected versions of the signal of distinct signal strengths, phases and delays being received. This delay between the different received signals causes inter-symbol interference (ISI). In an OFDM system the CP [5] is used to mitigate these ISI effects.

This can be thought of as trying to communicate with a person at the end of a long cave. If one continuously yells without pausing, the person at the end of the cave will be unable to reconstruct the message because of the echoes (reflections). However, if each word (transmission) is separated by a pause of a few seconds, the echoes die away before the next word is spoken and the listener can hear each word. A CP insertion is seen to represent this

pause between transmissions or in this analogy, to let the echoes die away. A CP is amended to the beginning of the useful information of the signal. If zeros were sent in the CP, this would cause the radio frequency (RF) power amplifier to switch on and off and this might cause unwanted spectral output [5]. This interval can still be used to represent pauses in the transmission at the receiver if known signals are sent in this interval. As shown in Fig. 2.5,

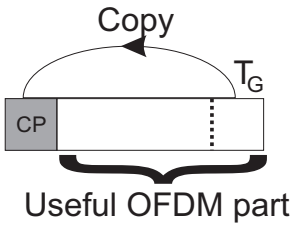

Figure 2.5: Cyclic prefix insertion

a CP is generated by amending a portion of the end of a signal to the front of the signal. Depending on the channel, an OFDM signal $T_x(t)$ linearly convolves with the channel $H(t)$ (e.g. the PDP in Fig. 2.4(b)) during its transmission. However an equaliser requires circular convolution [6] $T_x(t) \star H(t)$ in the time-domain, which is equivalent to multiplication in the frequency domain $t_x(f) \cdot h(f)$. Here $t_x(f)$ is a frequency-domain representation of the signal and $h(f)$ is the channel transfer function. A linearly convolved signal is different from a circularly convolved signal [6]. An equaliser will later use this circularly convolved relationship ($t_x(f) \cdot h(f)$) to mitigate the effects of the channel.

In order to achieve circular convolution a CP is inserted, i.e. a portion of the end of a signal is amended to the front of the signal. After adding a CP to $T_x(t)$ and transmitting the signal through the channel ($H(t)$), the desired circular convolution $T_x(t) \star H(t)$ may be achieved, provided the CP is of sufficient length, and the received signal removes the CP. The transmitted signal encounters both channel effects H(t) and additive white Gaussian noise (AWGN) denoted by $n(t)$. The subsequent received signal can be written as

$$R_x(t) = T_x(t) \cdot H(t) + n(t). \tag{2.5}$$

2.4 OFDM RECEIVER

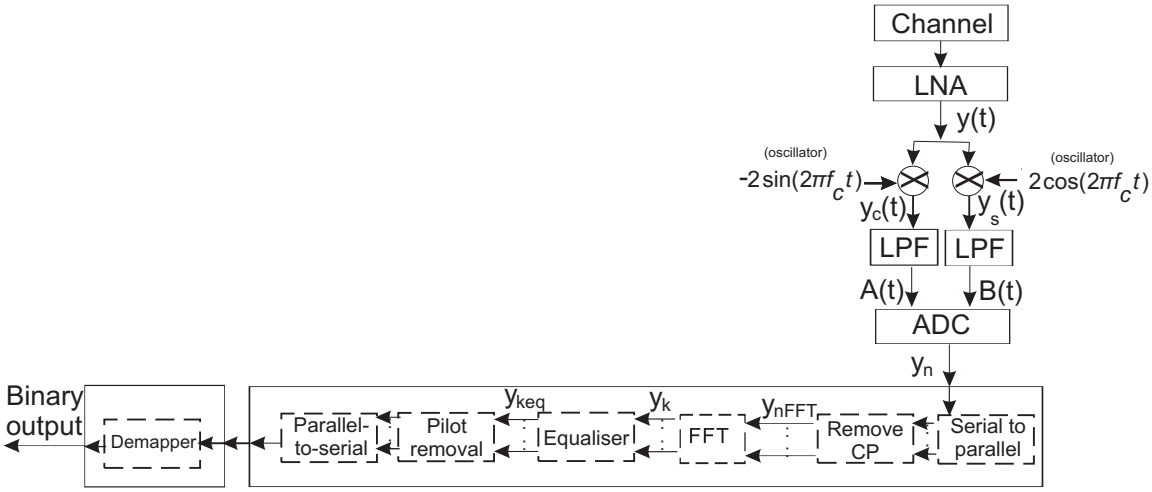

Figure 2.6: Orthogonal frequency division multiplexing receiver structure

At the receiver [2], as depicted in Fig. 2.6, the incoming signal is passed through a low-noise amplifier (LNA). In the case of a linear amplification process with an amplification factor of a, the output can be written as

$$\begin{aligned} y(t) &= (T_x(t)\cdot H(t)+n(t))\cdot a \\ &= m(t)\cdot \check{H}(t)+\check{n}(t). \end{aligned} \tag{2.6}$$

In Eq (2.6), $\check{H}(t) = A\cdot H(t)\cdot a$ and $\check{n}(t) = n(t)\cdot a$. Thereafter the signal is multiplied by a co-sinusoid and a sinusoid; this results in

$$\begin{aligned} y_c(t) &= 2\left(\frac{1}{\sqrt{N}}\sum_{k=0}^{N-1}\check{H}(t)\cdot(a_k\cos(2\pi f_c t+\omega_k t)-b_k\sin(2\pi f_c t+\omega_k t))+\check{n}(t)\right)\cdot\cos(2\pi f_c t) \\ &= \frac{1}{\sqrt{N}}\sum_{k=0}^{N-1}\Big(\check{H}(t)\cdot a_k\cos(\omega_k t)+\check{H}(t)\cdot a_k\cos(4\pi f_c t+\omega_k t)-\check{H}(t)\cdot b_k\sin(4\pi f_c t+\omega_k t) \\ &\quad -\check{H}(t)\cdot b_k\sin(\omega_k t)\Big)+\cos(2\pi f_c t)\cdot\check{n}(t) \end{aligned} \tag{2.7}$$

and

$$y_s(t) = -2\left(\frac{1}{\sqrt{N}}\sum_{k=0}^{N-1}\check{H}(t)\cdot(a_k\cos(2\pi f_c t+\omega_k t)-b_k\sin(2\pi f_c t+\omega_k t))+\check{n}(t)\right)\cdot\sin(2\pi f_c t)$$

$$= \frac{1}{\sqrt{N}}\sum_{k=0}^{N-1}\Big(-\check{H}(t)\cdot a_k\sin(4\pi f_c t+\omega_k t)+\check{H}(t)\cdot a_k\sin(\omega_k t)+\check{H}(t)\cdot b_k\cos(\omega_k t)$$
$$-\check{H}(t)\cdot b_k\cos(4\pi f_c t+\omega_k t)\Big)-\sin(2\pi f_c t)\cdot\check{n}(t). \tag{2.8}$$

The low pass filter (LPF) removes the high-frequency components ($4\pi f_c t$). This results in

$$\begin{aligned} A(t) &= \frac{1}{\sqrt{N}}\sum_{k=0}^{N-1}\Big(\check{H}(t)\cdot a_k\cos(\omega_k t)-\check{H}(t)\cdot b_k\sin(\omega_k t)\Big)+\cos(2\pi f_c t)\cdot\check{n}(t) \\ &= \frac{1}{\sqrt{N}}\sum_{k=0}^{N-1}\Big(\check{H}(t)\cdot a_k\cos(\omega_k t)-\check{H}(t)\cdot b_k\sin(\omega_k t)\Big)+\check{n}_c(t) \end{aligned} \tag{2.9}$$

and

$$\begin{aligned} B(t) &= \frac{1}{\sqrt{N}}\sum_{k=0}^{N-1}\Big(\check{H}(t)\cdot a_k\sin(\omega_k t)+\check{H}(t)\cdot b_k\cos(\omega_k t)\Big)-\sin(2\pi f_c t)\cdot\check{n}(t) \\ &= \frac{1}{\sqrt{N}}\sum_{k=0}^{N-1}\Big(\check{H}(t)\cdot a_k\sin(\omega_k t)+\check{H}(t)\cdot b_k\cos(\omega_k t)\Big)-\check{n}_s(t) \end{aligned} \tag{2.10}$$

where $\check{n}_c(t)$ and $\check{n}_s(t)$, refer to the noise components. The resultant signal is passed through an analog-to-digital converter (ADC), thus $t=\frac{nT_s}{N}$ and $\omega_k=\frac{2\pi k}{T_s}$. Thereafter the real components (Eq (2.9)) and the imaginary components (Eq (2.10)) are placed in a complex form given by

$$\begin{aligned} y_n &= (A_n+j\cdot B_n)+n_c s \\ &= \frac{1}{\sqrt{N}}\sum_{k=0}^{N-1}\check{H}_n\cdot\left(a_k\cos\left(\frac{2\pi nk}{N}\right)-b_k\sin\left(\frac{2\pi nk}{N}\right)\right) \\ &\quad +j\cdot\left(a_k\sin\left(\frac{2\pi nk}{N}\right)+b_k\cos\left(\frac{2\pi nk}{N}\right)\right)+n_c s \\ &= \frac{1}{\sqrt{N}}\sum_{k=0}^{N-1}\check{H}_n\cdot\left((a_k+jb_k)\cdot\left(\cos\left(\frac{2\pi nk}{N}\right)+j\cdot\sin\left(\frac{2\pi nk}{N}\right)\right)\right)+n_c s \\ &= \frac{1}{\sqrt{N}}\sum_{k=0}^{N-1}\check{H}_n\cdot X_k e^{j\frac{2\pi nk}{N}}+n_{cs}. \end{aligned} \tag{2.11}$$

In Eq (2.11), n_{cs} represents complex noise, $\check{H}_n$ is a discrete representation of the channel, A_n

and B_n are discrete ($t = \frac{nT_s}{N}$) representations of Eq (2.9) and Eq (2.10), respectively. This signal is similar to the initially transmitted signal Eq (2.1). The subsequent discrete signal undergoes a serial-to-parallel conversion and is passed into the CP removal unit. Provided the CP is of a sufficient length and the CP is removed, the input into the fast Fourier transform (FFT) can be written as

$$y_{nFFT} = \frac{1}{\sqrt{N}} \sum_{k=0}^{N-1} \check{H}_n \star X_k e^{j\frac{2\pi nk}{N}} + n_{cs}. \tag{2.12}$$

The FFT maps the OFDM symbols $[X_0, X_1, ...X_{N-1}]$ to constellation symbols $[x_0, x_1, ...x_{N-1}]$. The output of the FFT can be written as

$$y_k = h_k \cdot x_k + \eta_k \qquad k = 0, ..., N-1 \tag{2.13}$$

where h_k, is the channel impulse response and η_k is additive noise. At the output of the FFT, an equaliser estimates the channel effects ($\hat{h_k}$). This estimate is based on comparing the transmitted pilot symbols x_{ks} (which are known at the receiver) with the received pilot symbols y_{ks} ($\hat{h_k} = \frac{y_{ks}}{x_{ks}}$) and thereafter interpolating such that a channel estimate $\hat{h_k}$ can be obtained. Thereafter the channel effects can be mitigated by an equaliser as indicated below

$$\begin{aligned} y_{keq} &= \frac{h_k \cdot x_k + \eta_k}{\hat{h_k}}, \qquad k = 0, 1, ...N-1 \\ &\approx x_k + n_k \end{aligned} \tag{2.14}$$

where n_k refers to noise. The pilot symbols are removed and a parallel-to-serial conversion is performed. The symbols are de-mapped, resulting in the received binary data.

2.5 BRIEF HISTORY OF OFDM

The first OFDM-like radio found in the literature was the Kineplex system [7], developed in 1958. This radio used 20 tones, each differentially phase modulated and separated by 110 Hz with a total approximate bandwidth of 3400 Hz. Thereafter, a military radio called KATHRYN was developed in 1967 [8]. KATHRYN used 34 parallel phase modulated channels with a 82 Hz spacing. In 1968, ANDEFT [9] was created, this modem used 66 frequency

differentially phase modulated tones, each separated by 40 Hz. Theoretical contributions to the development of OFDM were made by B. R. Saltzberg [10] in 1967 and R. W. Chang [11] in 1968. Thereafter, Chang in 1970 obtained a US patent [12] for OFDM. Saltzberg in the same year obtained a patent [12] for an orthogonal transmission system. In 1971 Weinstein and Ebert [13] suggested using a discrete Fourier transform (DFT) for orthogonal sub-carrier placement. In 1985 Cimini [14], suggested using OFDM for wireless communication.

In the 1990's the work of J. M. Cioffi et al. [15–18], led to the acceptance of OFDM in the digital subscriber lines standards. It was the computational complexity required to implement the DFT, that had halted the implementation until the 1990's. Ever since then, OFDM has been used in various standards such as DVB, DRM, WiMAX, Wi-Fi and recently in LTE. However, no technology is perfect and OFDM is no different. A major problem associated with an OFDM transmission is its large PAPR. This high PAPR reduces the efficiency of the amplifiers, which is not desirable.

2.6 PEAK-TO-AVERAGE POWER RATIO

As previously mentioned, the sinusoidal signals of the sub-carriers of an OFDM transmission are given by

$$m(t) = \frac{1}{\sqrt{N}} \sum_{k=0}^{N-1} \left(a_k \cos(2\pi f_c t + \omega_k t) - b_k \sin(2\pi f_c t + \omega_k t) \right). \tag{2.15}$$

These series of sinusoidal signals add constructively, resulting as depicted in Fig. 2.7, in an OFDM transmission which consists of a number of infrequent peaks. This OFDM signal with infrequent peaks needs to be amplified before transmission through a channel.

This amplification process can be represented by Fig. 2.8(a). In this figure the blue curve is called the ideal gain characteristic of the amplifier, and the slope/gradient of this curve typically dictates the amount by which the incoming signal will be amplified. In practice, however, a typical gain curve indicated in green will be encountered. Ideally the amplifier should operate in the linear region of the gain curve, such that an exact amplified

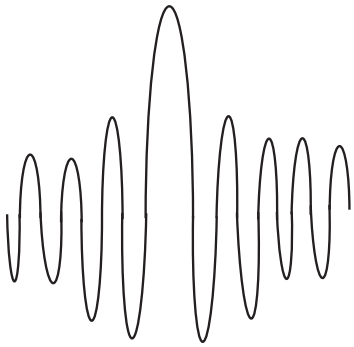

Figure 2.7: OFDM time-domain signal representation

output of the input signal is produced.

In Fig. 2.8(a), the bottom (black) input is an OFDM signal, which needs to be amplified and the output is represented by the (red) amplified OFDM signal, which is transmitted across the channel. For this type of OFDM signal, depicted in Fig. 2.8(a), the power amplifier would on average operate (at the red point) far below the optimum operating point (purple point). The power amplifier is powered up to just above the optimum operating point. However, on average, the amplifier is operated far below (at the red point) the optimum operating point. The region between these two points (optimum operational and average operational point) is reserved for amplification of the irregular peak values of an OFDM transmission.

On the contrary, for a sinusoid signal, depicted in Fig. 2.8(b), the power amplifier would on average operate just below (red point) the optimum operating point. This is closer to the optimum operating point than its OFDM counterpart. As previously mentioned, an OFDM signal backs off from its optimum operating point in order to accommodate the peaks of the signal. If a sufficient back-off were not present, as shown Fig. 2.8(c), the incoming signal would operate outside of the linear region of the amplifier. This would result in clipping and a subsequent BER degradation. For illustration purposes the optimum operating points and average operating points, from Fig. 2.8(a) and Fig. 2.8(b), are placed in Fig. 2.9. This represents the power efficiency characteristic curve of a standard off-the shelf (OTS) class AB amplifier. In Fig. 2.9 the y-axis indicates the power amplifier efficiency and

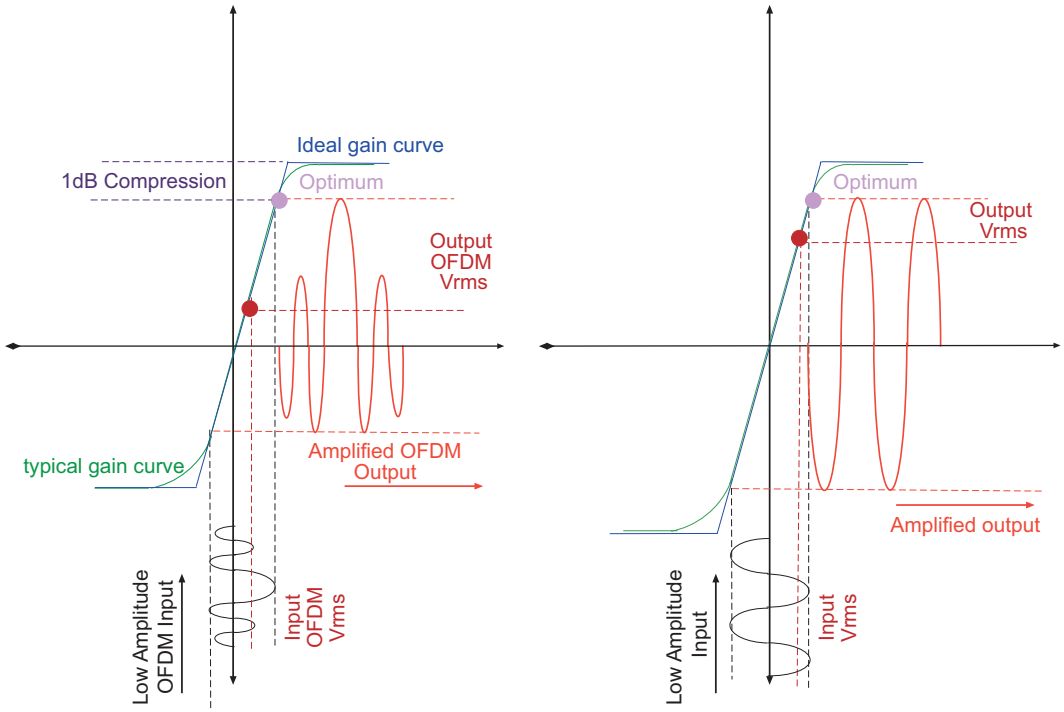

(a) OFDM amplification

(b) Sinusoid amplification

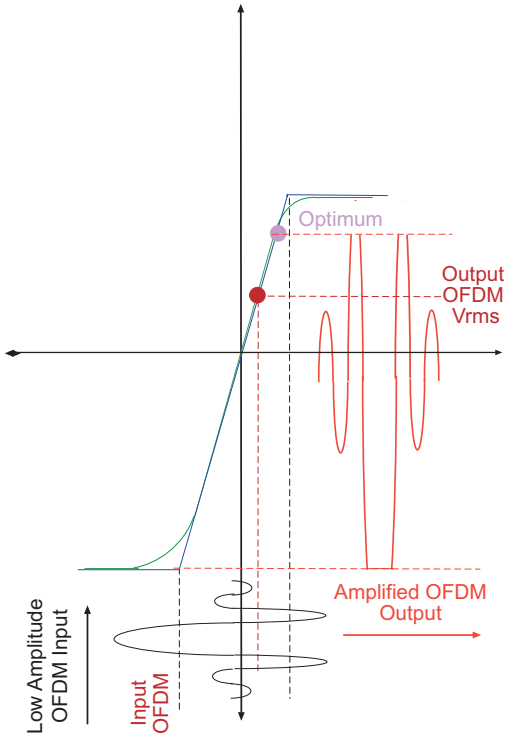

(c) Clipped OFDM amplification

Figure 2.8: An amplification process depiction

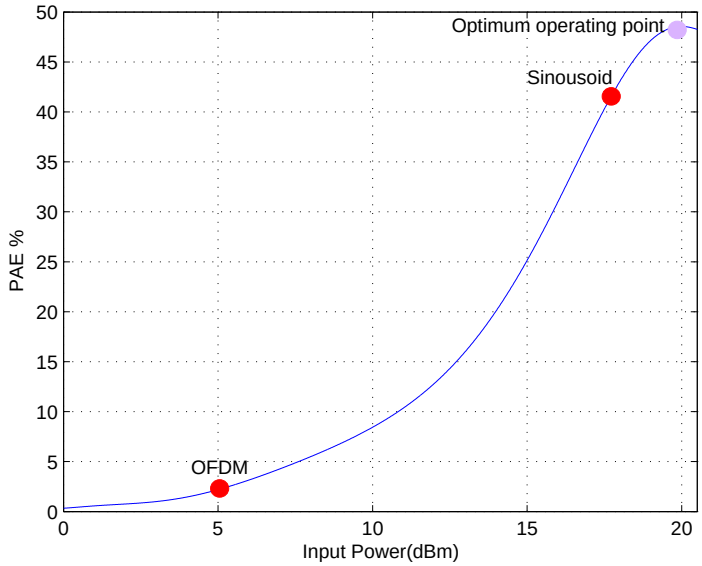

Figure 2.9: Typical power efficiency characteristics of a standard off-the shelf amplifier

the x-axis represents the average input power. From this illustration, when operating the amplifier in the upper regions, it is evident that the amplifier's efficiency is roughly 48%.

In the lower regions, this efficiency exponentially decays to only a few percent. In Fig. 2.9 it is seen that the sinusoid transmission is a more power-efficient transmission than its OFDM counterpart, which has an efficiency of a few percent. It is this inefficient use of the amplifier, due to the nature of the OFDM signal, which ultimately reduces the battery of a mobile device. An indication of the efficiency at which an amplifier is being operated can be obtained by using the PAPR term. The PAPR of a particular base band transmission is commonly defined as [19]

$$\text{PAPR}\{m_n\} = \max_{0\leq n<NL-1} \frac{|m_n|^2}{\text{E}\{|m_n^2|\}}. \tag{2.16}$$

In Eq (2.16), m_n refers to the signal of interest, N refers to the number of sub-carriers, L is the oversampling factor and $E\{\cdot\}$ is the expected value. For a sinusoidal transmission, depicted in Fig. 2.8(b), the PAPR is 3 dB [20], this indicates that the power amplifier is being used reasonably efficiently. Similarly, for an OFDM transmission, depicted in Fig. 2.8(a), the PAPR could be approximately 12 dB [21]. As the PAPR value of the transmission increases

as suggested in Fig. 2.9, the power amplifier efficiency exponentially decreases.

2.7 PEAK ENVELOPE POWER

Another term, called peak envelop power (PEP) is used to describe the characteristics of a particular transmission. The PEP of a complex pass band signal $m(t)$ is defined as [22]

$$\text{PEP}\{m(t)\} = \max|m(t)|^2. \tag{2.17}$$

PEP represents the maximum power of a complex baseband signal $m(t)$.

2.8 A LITERATURE REVIEW OF VARIOUS PAPR METHODS

Various methods [19, 22, 23] have been suggested to reduce the PAPR. These include clipping [19, 22–32], decision-aided reconstruction clipping [28], coding [23, 33–42], partial transmission sequence [22, 43–51], selective mapping [22, 52–58], companding transforms [59–67], active constellation extension [68–74], tone reservation [23, 75–81] and CE-OFDM [82–90], amongst others.

2.8.1 Clipping

Clipping [19, 22–32] is the simplest method of reducing the PAPR, as demonstrated in Fig. 2.8(c), by limiting the peak amplitude level of the input signal to a predetermined level. This clipping process is commonly denoted by [22]

$$m(t)^c = \begin{cases} -\text{A} & m(t) \leq -\text{A} \\ m(t) & |m(t)| < \text{A} \\ \text{A} & m(t) \geq \text{A}. \end{cases} \tag{2.18}$$

In Eq (2.18), $m(t)^c$ is the clipped OFDM transmission, $m(t)$ represents the OFDM transmission and A is the predetermined amplitude level. When classically clipping a signal (Fig. 2.10), at various clipping ratios, both in-band and out-of-band distortions are intro-

duced. Where the clipping ratio (CR) is defined as [22]

$$\text{CR} = \frac{A}{V_{rms}} \tag{2.19}$$

here, V_{rms} is the root mean square (RMS) value of the OFDM transmission. In order to minimise the in-band distortion, the classically clipped OFDM signal needs to be oversampled. To limit the out-of-band distortion, the clipped OFDM signal, depicted in Fig. 2.11, is filtered before transmission. The resultant filtered transmission is depicted in Fig. 2.12.

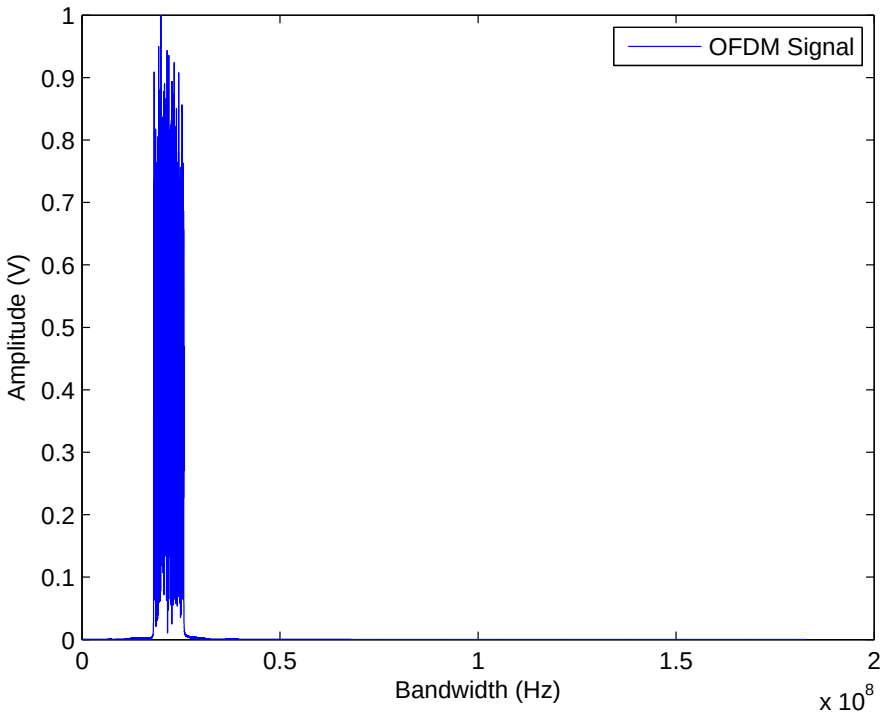

Figure 2.10: Normalised OFDM transmission

At the receiver, the clipped samples can be reconstructed by using a number of methods [19, 23, 27, 28].

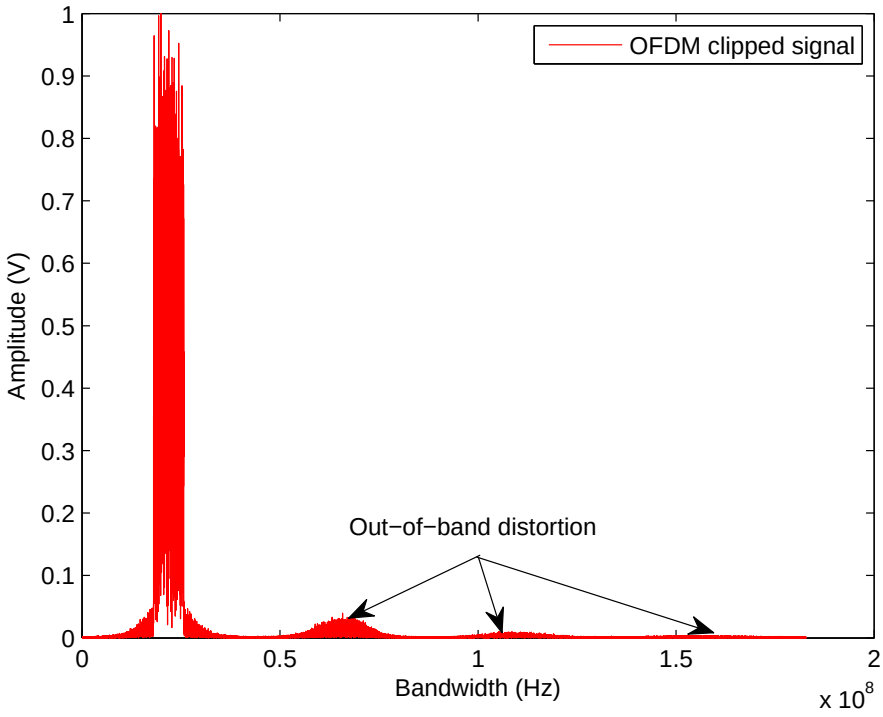

Figure 2.11: Normalised clipped OFDM transmission

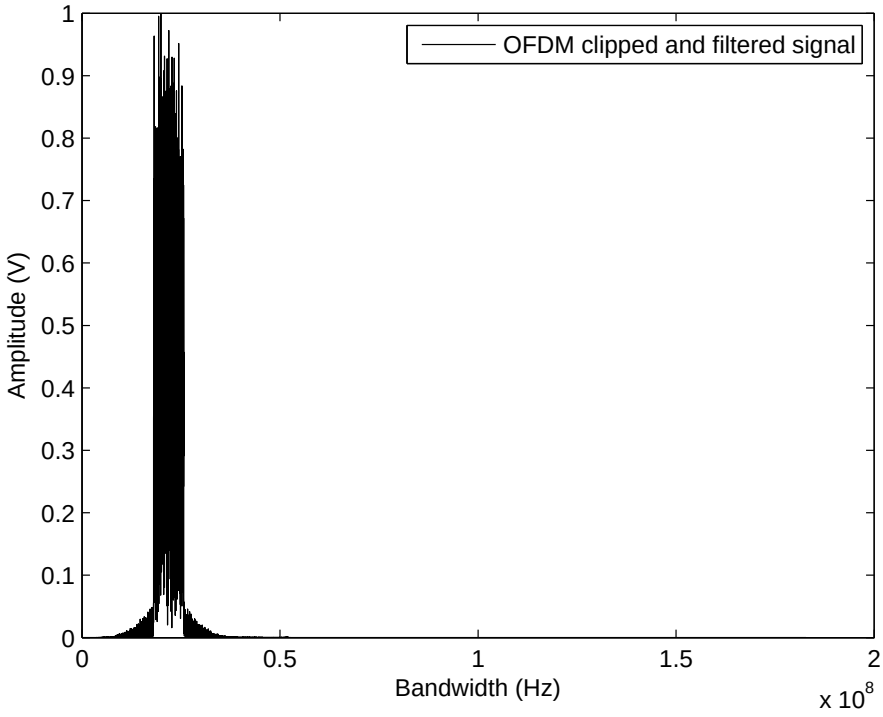

Figure 2.12: Normalised clipped and filtered OFDM transmission

Kim [28] has recommended using an iterative process called decision-aided reconstruction (DAR) clipping to reconstruct the clipped signal. During the DAR process, as depicted in

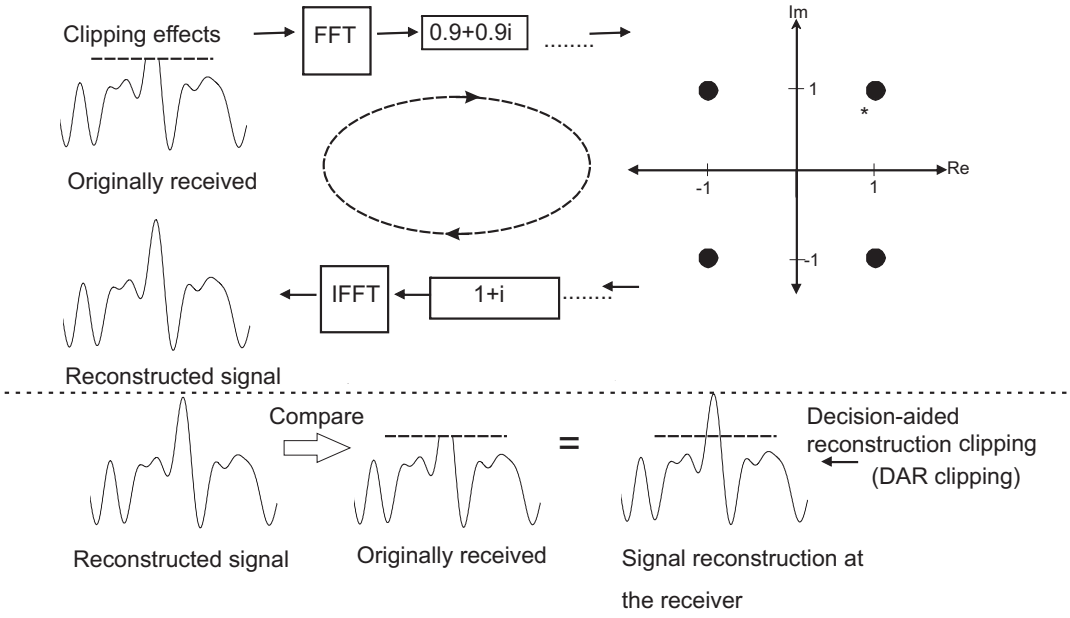

Figure 2.13: Decision-aided reconstruction process

Fig. 2.13, the received clipped OFDM signal is passed through a traditional OFDM receiver process. The received noisy clipped symbols (e.g. $0.9+0.9\text{i}, \ldots$) are compared to a set of known transmitted symbols (e.g. $1+\text{i}$, $1-\text{i}$, $-1-\text{i}$ and $-1+\text{i}$); where the most likely symbols (e.g. $1+\text{i}$, ...) are selected as the possible original symbols. These newly selected symbols (e.g. $1+\text{i}$, ...) are passed through the OFDM transmission process to produce a reconstructed OFDM signal. The originally received signal and reconstructed signals are compared. The receiver is assumed to have knowledge of the clipping threshold. By using this knowledge in regions above the clipping threshold, a DAR clipped signal is produced by amending the reconstructed signal to the originally received signal.

This DAR clipped signal is passed through an OFDM receiver process and thereafter through the OFDM transmission process. The subsequently reconstructed signal is compared to the originally received OFDM signal. With knowledge of this clipping threshold, further amendments are made to the originally received OFDM signal. This process is iteratively continued until convergence is reached. A limiting factor of clipping, as well as DAR clipping, is that as the number of peak amplitudes increases, this leads to a severe

degradation. Furthermore, the iterative nature of the DAR technique requires increased computational complexity. In addition, the DAR method is not suitable for real world frequency selective fading conditions.

2.8.2 Coding

In contrast to clipping, coding [23, 33–42] can also be used to reduce the PAPR, by selecting a codeword which minimises the PAPR. Various coding schemes have been recommended by Jiang [23] and Jones [34]. Jones [34], as shown in Fig. 2.14, has recommended using a block encoding scheme to reduce the PAPR of a transmission. During this process, depicted

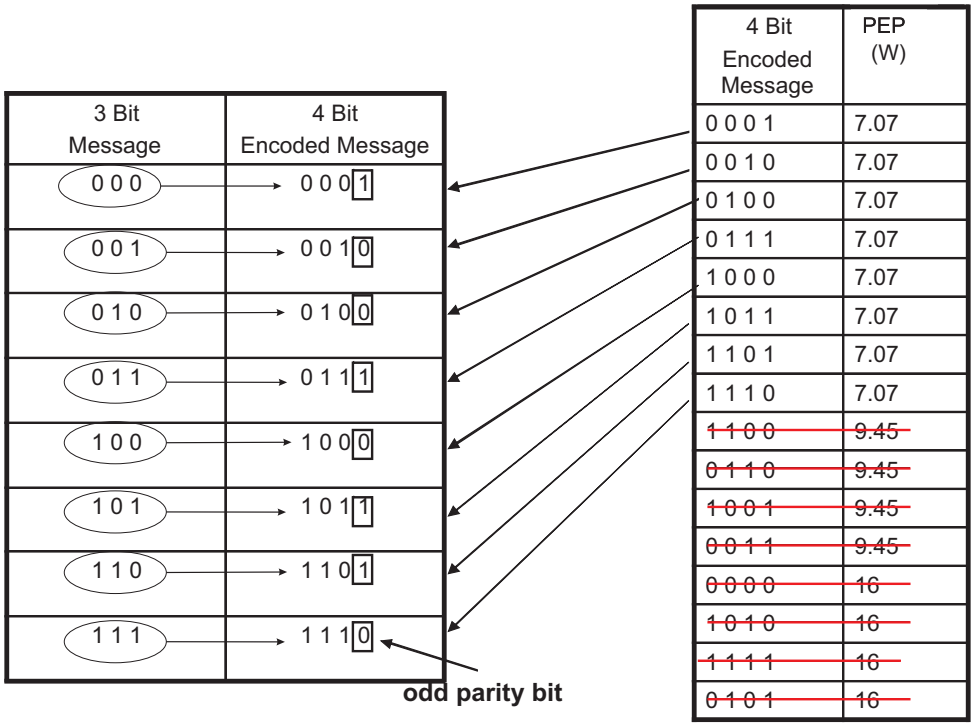

Figure 2.14: Coding

in Fig. 2.14, each 3-bit message will be encoded onto a 4-bit encoded message. All possible 4-bit encoded messages, as well as their subsequent PEP, are determined. All 4-bit encoded messages with large PEPs are eliminated. The 3-bit message is mapped onto the remaining low PEP 4-bit encoded message. In this particular case, for the 4-bit encoded message, the first 3-bits of the codeword and message are the same; the fourth bit is used as an odd parity check bit to determine the presence of an error in the transmission. An error in transmission

is observed if the received encoded message does not contain either three 1's or three 0's. Davis [33] has further shown that it is possible to combine block coding (with its encoding, decoding and error-correcting capability) and Golay complementary sequences (with their attractive PAPR properties), to reduce the PAPR. Coding can reduce the PAPR; however, it is not always possible to achieve a specific PAPR value. In certain cases coding gain is sacrificed for this PAPR decrease. In addition, an exhaustive search for good codewords for an OFDM system with a large number of carriers is difficult.

2.8.3 Partial transmitted sequence

An alternative method, employed in PAPR reduction, is the partial transmitted sequence (PTS) [22, 43–51] technique. In this PTS technique, depicted in Fig. 2.15, the input data block of N symbols is partitioned into V disjointed equally sized sub-blocks, which can be written as [22]

$$x = [x_1, x_2, x_3 \ldots\ldots, x_V]^T. \tag{2.20}$$

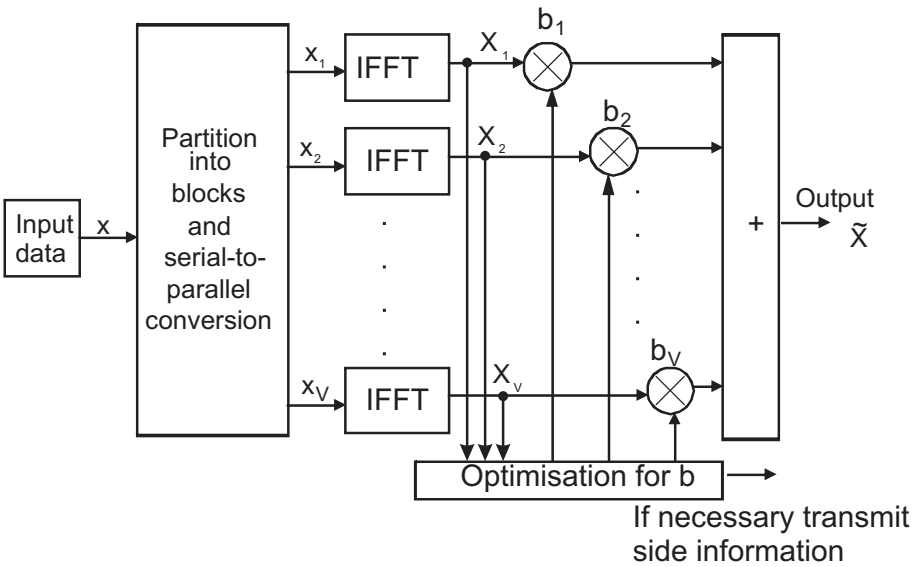

Figure 2.15: Partial transmitted sequence [22]

These sub-blocks are inverse fast Fourier transformed. Thereafter, each partitioned sub-block

is multiplied by a corresponding complex phase rotation factor $b_v = e^{j\phi v}$, $v = 1,2,....V$ to yield

$$\tilde{X} = \sum_{v=1}^{V} b_v \cdot IFFT\{x_v\} = \sum_{v=1}^{V} b_v \cdot X_v. \tag{2.21}$$

The objective of this phase rotation is to combine these sub-blocks optimally to achieve a minimum PAPR. The phase rotation factor is chosen such that [43]

$$[b_1, b_2...., b_V] = \arg\min_{[b_1,b_2....,b_V]} \left(\max_{n=0,1....N-1} \left| \sum_{v=1}^{V} b_v \cdot X_v \right| \right). \tag{2.22}$$

A limiting factor of PTS is that it requires high computational overhead to find an optimum phase-rotated sub-block combination and requires additional side information to be transmitted to allow the receiver to reconstruct the original signal.

2.8.4 Selective mapping

In selective mapping (SLM) [22,52–58], depicted in Fig. 2.16, the input data block is mapped onto different candidate data blocks, all representing the same information as the original data block. These subsequent mapped data blocks are inverse fast Fourier transformed and the data transmission with the lowest PAPR is selected for transmission.

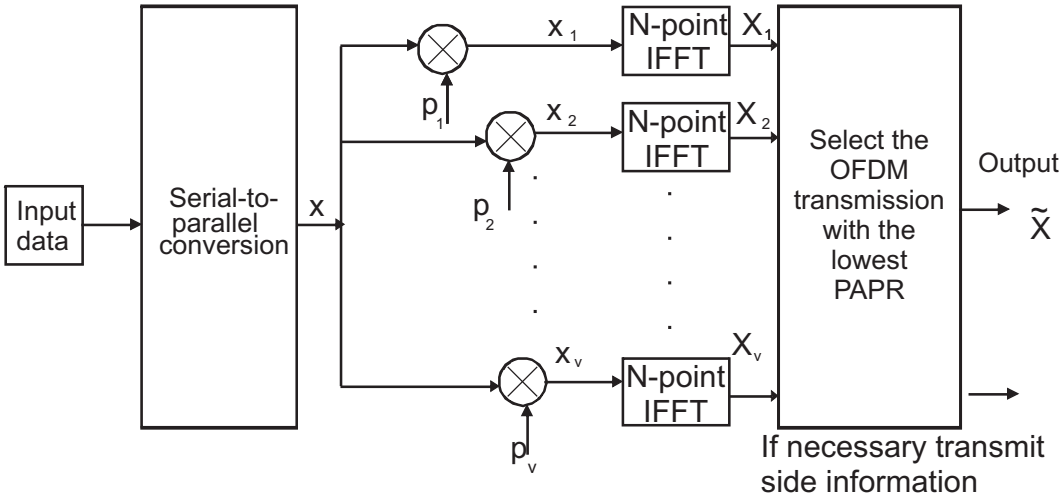

Figure 2.16: Selective mapping [22]

For a SLM transmission the input data block, given by [52]

$$x = [x_1, x_2, x_3 \ldots\ldots\ldots, x_N] \tag{2.23}$$

is multiplied by v different phase sequences each of length N. These phase sequences can be written as

$$\begin{aligned} p_V &= [p_{\{V,1\}}, p_{\{V,2\}}, p_{\{V,3\}} \ldots\ldots\ldots, p_{\{V,N\}}]^T && (2.24) \\ &= [e^{j\phi_{\{V,1\}}}, e^{j\phi_{\{V,2\}}}, e^{j\phi_{\{V,3\}}} \ldots\ldots\ldots, e^{j\phi_{\{V,N\}}}]^T. && (2.25) \end{aligned}$$

In Eq (2.24), $V = 1, 2, 3 \ldots\ldots v$, $\phi_{\{V,1\}}, \phi_{\{V,2\}} \ldots\ldots\ldots \phi_{\{V,N\}} \in [0, 2\pi)$. This multiplication of Eq (2.23) with Eq (2.24) produces modified data blocks, all representing the same information as the original data block given by

$$x_V = [x_{\{V,1\}}, x_{\{V,2\}}, x_{\{V,3\}} \ldots\ldots\ldots, x_{\{V,N\}}]^T, \tag{2.26}$$

where as previously mentioned $V = 1, 2, 3 \ldots\ldots v$. The subsequent signals in Eq (2.26) are passed through an IFFT and thereafter, the transmission with the lowest PAPR is selected for transmission.

Just as in the case of PTS, this method requires high computational overhead, as well as the transmission of side information. Various authors [54, 55, 57] have proposed methods of reducing the computational complexity, while Breiling [53] has suggested a method which does not require the transmission of side information. In addition, various methods [44–46, 48–50] have been recommended to reduce the complexity of the PTS method. Despite all of these methods, both PTS and SLM still require relatively high computational overhead and in some cases the transmission of side information.

2.8.5 Companding

Another method employed in PAPR reduction involves using a companding transform [59–67]. Wang [59] has proposed using a non-linear transform, illustrated in Fig. 2.17, which

enlarges the small signals while compressing the large signals. The idea behind non-linear companding transforms originates from speech processing. Similar to speech signals, OFDM signals contain peaks which occur irregularly, thus similar companding techniques to those used in speech processing may be applied to improve the PAPR of an OFDM transmission.

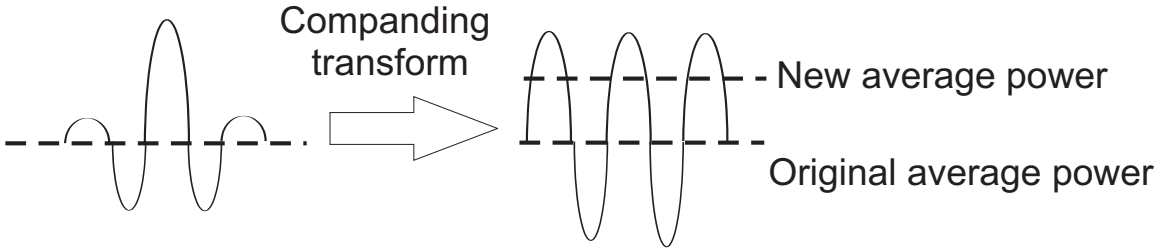

Figure 2.17: Depiction of a companding transform

The design criteria for a non-linear companding transform that can be used on an OFDM signal have been discussed in [66]. With knowledge of both the distribution of an OFDM signal (for instance a Rayleigh distribution) and a desired distribution of a companded OFDM signal, a non-linear companding transform function can be obtained through theoretical analysis. For example, suppose an original OFDM signal is required to have a desirable probability density function of $f(s) = ks + b \quad (k < 0, b > 0)$. The non-linear companding function which can be used for this type of distribution is given by [66]

$$C(x) = \sqrt{6}\sigma\left[1 - e^{-\frac{x^2}{2\sigma^2}}\right]. \tag{2.27}$$

In Eq (2.27), x refers to the input OFDM signal and σ is the variance of the OFDM signal. Huang [62] has also proposed a companding method based on μ law companding, which combined clipping and Wang companding, to reduce the PAPR of OFDM signals. In addition, Jiang [61] has proposed an alternative companding technique, which uses the statistical distribution of an OFDM transmitted signal to reduce the PAPR. These companding methods increase the average power, as indicated in Fig. 2.17, of the signal and require larger linear amplifiers. Furthermore, by physically changing the appearance of an OFDM signal, some of the attractive OFDM signal properties are removed. This in turn results in a BER degradation.

2.8.6 Active constellation extension

A further PAPR reduction method is active constellation extension [68–74]. The ACE method, as depicted in Fig. 2.18, makes use of an iterative filtering and clipping process. As previously mentioned when classically clipping a signal at various clipping ratios, both in-band and out-of-band distortions are introduced.

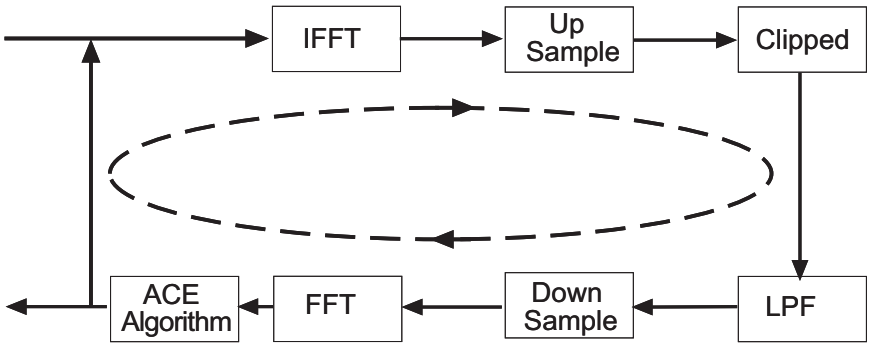

Figure 2.18: Active constellation extension method

For the ACE method, as depicted in Fig. 2.18, an up-sampled OFDM signal (after the IFFT) is clipped and filtered. The resultant signal is thereafter down-sampled and passed through a FFT. For a 16-QAM constellation after the FFT, depicted in Fig. 2.19(a), the resultant noise introduced by the clipping process is presented.

The outer constellation points of this clipped and filtered signal, which lies within a certain region that does not affect the BER, are left unaltered, hence the constellation is said to be extended [68]. As depicted in Fig. 2.19(b), the remaining constellation points are returned to their original position, before the clipping and filtering process. This process is iteratively continued.

Extending the outer constellation points leads to an average power increase. Generally the outer constellation points have a maximum tolerable constellation extension limit. Various projection methods [69, 71, 73] (e.g. projection onto convex sets approach) have been recommended to assist with this constellation shaping. Extending the outer

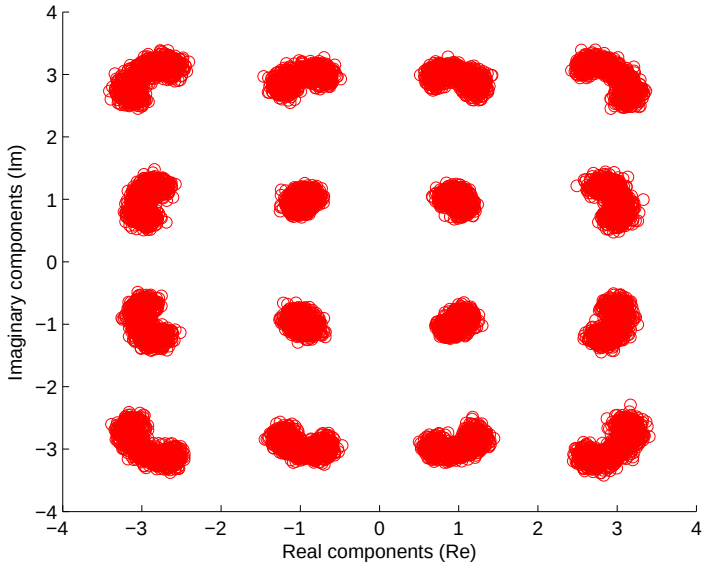

(a) Clipped and filtered OFDM constellation

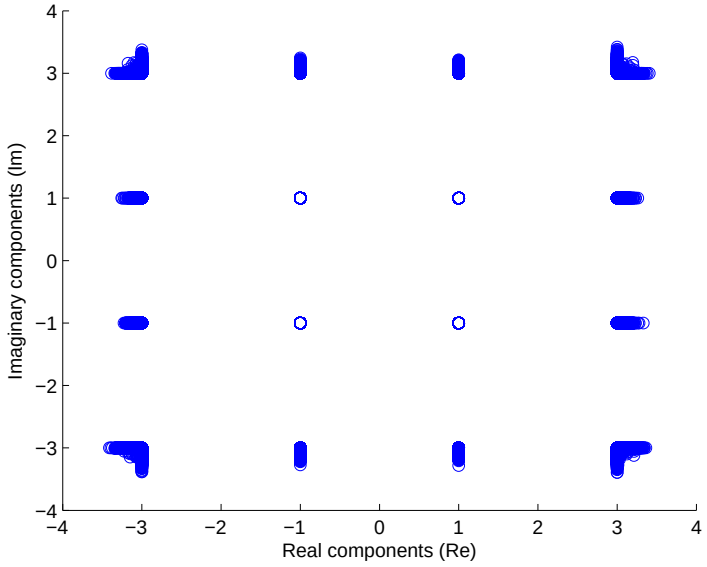

(b) Active constellation extension constellation

Figure 2.19: Constellation extension

constellation points leads to an average power increase and an average energy per bit increase. Furthermore, extending the constellation intelligently requires the use of an iterative clipping process. The iterative nature of this process increases the computational complexity. In addition, the optimum choice of clipping parameters may prove difficult and it is not always possible to achieve a specific PAPR value.

2.8.7 Tone reservation

An alternate method employed during PAPR reduction is tone reservation (TR) [23, 75–81]. With TR, the transmitter does not send data on a specified set of sub-carriers. The objective of TR is to find a time-domain signal c which can be added to the original OFDM time-domain signal x, such that the PAPR is reduced. This can be accomplished by adding a frequency-domain vector [75]

$$C = [C_0, C_1 ..... C_{N-1}]^T \tag{2.28}$$

to a frequency domain OFDM vector X; the new time domain signal can be written as

$$x + c = IFFT\{X + C\}. \tag{2.29}$$

The peak reduction vector C lies in a disjointed subspace i.e.

$$X_n = 0, n \in \{i_1, i_2, i_3, ...i_l\} \text{ and } C_n = 0, \notin \{i_1, i_2, i_3, ...i_l\}. \tag{2.30}$$

The l non-zero positions in vector C are called peak reduction carriers. These C subcarriers are orthogonal to X and cause no distortion on the data-bearing subcarriers. The C subcarriers may be obtained as suggested by [75], as depicted in Fig. 2.20, by clipping and filtering an up-sampled OFDM signal (after the IFFT containing TR symbols). The resultant signal is thereafter down-sampled and passed through an FFT. The resultant noise introduced by the clipping and filtering process (after the FFT) is mapped onto the TR symbols and the remaining symbols are left unaltered.

Similar to the ACE method, the iterative nature of the TR process increases the computational complexity and finding the optimum choice of the clipping parameter may prove difficult. Furthermore, the reservation of sub-carriers compromises throughput and it is not always possible to achieve a specific PAPR value.

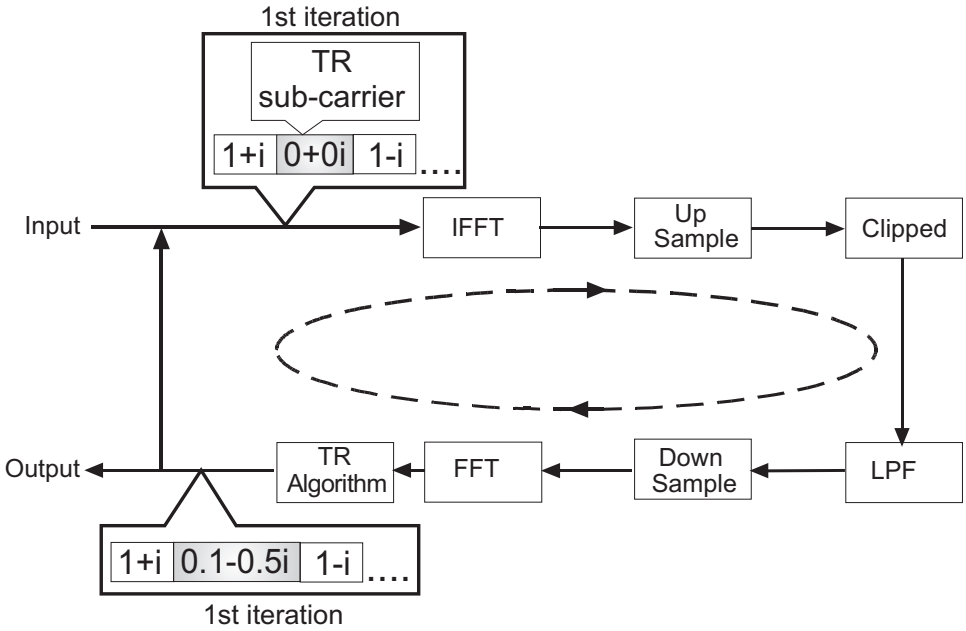

Figure 2.20: Tone reservation scheme

2.8.8 Constant envelope OFDM phase modulation

In contrast to tone reservation, constant envelope OFDM phase modulation [82–90] combines OFDM and phase modulation. A CE-OFDM transmission is ideally suited for constellations without imaginary components (e.g. BPSK). In cases where imaginary components exist (e.g. such as in 16-QAM), this constellation is uniquely mapped onto a constellation without imaginary components (e.g. 16-QAM to 16-PAM mapping). After the mapping process, an IFFT is performed on the mapped signal. The resultant OFDM signal is phase modulated. A drawback of CE-OFDM is its bandwidth expansion. Narrow band constraining of the transmission affects the BER of the system (the classical feature of a phase modulated signal). In addition, the mapping process affects the BER. In Chapter 4, an in-depth discussion of this method is provided.

2.9 CONCLUDING REMARKS

Ideally, a PAPR method that does not result in a number of the draw backs being experienced by current methods in the field is required. In Table 2.1, the disadvantages associated with the various methods are summarised. In this thesis, a method called offset modulation (OM-

Table 2.1: Disadvantages associated with the various PAPR reduction methods.

Methods	**Disadvantages**
Partial transmitted sequence Selective mapping DAR clipping Active constellation extension Tone reservation	High implementation complexity
Companding Active constellation extension Tone reservation	Leads to an increase in average power
Coding	Affects the coding gain
CE-OFDM Partial transmitted sequence Selective mapping Tone reservation	Requires further bandwidth expansion or the transmission of side information
Clipping DAR clipping CE-OFDM	Leads to a severe BER degradation as the number of carriers increases

OFDM) is proposed, which does not result in a number of the disadvantages summarised in Table 2.1.